Controlled Growth of a Single Palladium Nanowire between Microfabricated Electrodes

Mangesh A. Bangar,[†] Kumaran Ramanathan,[†] Minhee Yun,[‡] Choonsup Lee,[‡] Carlos Hangarter,[†] and Nosang V. Myung*,[†,§]

Department of Chemical and Environmental Engineering and Center for Nanoscale Science and Engineering, University of California−Riverside, Riverside, California 92521, and Jet Propulsion Laboratory, California Institute of Technology, Pasadena, California 91109

Received July 2, 2004. Revised Manuscript Received August 26, 2004

We report a novel electrochemical method for dimensionally controlled growth of a single palladium nanowire between premicrofabricated electrodes. In this method, the dimensions of the nanowire are defined by the dimensions of the e-beam-patterned channel between the microfabricated gold electrodes. The formation of the nanowire is confirmed by both optical and scanning electron microscopy imaging in addition to the electrical measurement using the two terminal current−voltage ($I-V$) characteristics of the nanowire. Fabrication of a single localized palladium nanowire with controlled dimensions is demonstrated for 100 nm, 500 nm, and 1 μm wide and 2.5 μm long channels (length-to-diameter ratio ~2.5−25). The growth profile, confinement, resistance, and morphology of the nanowires were strongly influenced by the deposition conditions. A current of −100 nA was found to provide well-confined, stable nanowires with ohmic contact with the gold electrodes.

Introduction

Controllable growth of stable metallic nanowires has been a topic of continuing investigation, because of the need to obtain high-performance high-density nanoelectronic devices including nanosensors. Various metallic nanowires including copper, nickel, gold, palladium,[1] bismuth,[2] manganese oxide,[3] antimony,[4] and platinum[5,6] have been fabricated using a variety of techniques such as mechanical methods,[7] electrochemical methods,[1,4,8−11] chemical vapor deposition,[12] metal organic chemical vapor deposition,[13] sputtering,[14] micro contact printing,[15] electron beam evaporation,[16] and molecular beam epitaxy/SNAP.[6]

In most of these techniques, the procedures/methods involved lack the controllability over the nanowire dimensions and are unable to position the nanowires in specific locations to create nanoelectronic devices. Typically, these techniques produce a bundle of nanowires, which can be grown within a specific template, e.g., alumina,[4] a polycarbonate membrane,[5] or an epitaxially grown gallium arsenide superlattice.[6] Alternately, a nanowire has been generated by stretching the bulk metal until atomic dimensions are achieved at the break point of the metallic wire.[7] Some of the methods also require postsynthetic modifications for constructing functional networks or devices such as nanowire alignment using an electric field[17] or fluidic arrangement of nanowires.[18] However, none of these techniques address the controllability of the nanowire growth/dimensions to obtain a "true" individually addressable nanowire(s). Recently, we have demonstrated a novel method to create individually addressable conducting polymer nanowires[19] and "micrometer/submicrometer" metallic nanowires[9] with good controllability of nanowire dimen-

* To whom correspondence should be addressed. E-mail: myung@engr.ucr.edu.

[†] Department of Chemical and Environmental Engineering, University of California−Riverside.

[‡] Jet Propulsion Laboratory, California Institute of Technology.

[§] Center for Nanoscale Science and Engineering, University of California−Riverside. California Institute of Technology.

(1) Walter, E. C.; Zach, M. P.; Favier, F.; Murray, B. J.; Inazu, K.; Hemminger, J. C.; Penner, R. M. *ChemPhysChem* **2003**, *4*, 131−138.

(2) Li, L.; Zhang, Y.; Li, G. H.; Zhang, L D. *Chem. Phys. Lett.* **2003**, *378*, 244−249.

(3) West, W. C.; Myung, N. V.; Whitacre, J. F.; Ratnakumar, B. V. *J. Power Sources* **2004**, *126*, 203−206.

(4) Zhang, Y.; Li, G.; Wu, Y.; Zhang, B.; Song, W.; Zhang, L. *Adv. Mater.* **2002**, *14*, 1227−1230.

(5) Husain, A.; Hone, J.; Postma, H. W. Ch.; Huang, X. M. H.; Drake, T.; Barbic, M.; Scherer, A.; Roukes, M. L. *Appl. Phys. Lett.* **2003**, *83*, 1240−1242.

(6) Melosh, N. A.; Boukai, A.; Diana, F.; Gerardot, B.; Badolato, A.; Petroff, P. M.; Heath, J. R. *Science* **2003**, *300*, 112−115.

(7) Xiao, X. Y.; Xu, B. Q.; Tao, N. J. *J. Am. Chem. Soc.* **2004**, *126*, 5370−5371.

(8) Li, C. Z.; He, H. X.; Bogozi, A.; Bunch, J. S.; Tao, N. J. *Appl. Phys. Lett.* **2000**, *76*, 1333−1335.

(9) Yun, M.; Myung, N. V.; Vasquez, R. P.; Menke, E.; Penner, R. M. *Nano Lett.* **2004**, *4*, 419−422.

(10) Favier, F.; Walter, E. C.; Zach, M. P.; Benter, T.; Penner, R. M. *Science* **2001**, *293*, 2227−2231.

(11) Li, C. Z.; Bogozi, A.; Huang, W.; Tao, N. J. *Nanotechnology* **1999**, *10*, 221−223.

(12) Dwivedi, D.; Dwivedi, R.; Srivastava, S. K. *Sens. Actuators, B* **2000**, *71*, 161−168.

(13) Lin, K. W.; Cheng, C. C.; Cheng, S. Y.; Yu, K. H.; Wang, C. K.; Chuang, H. M.; Chen, J. Y.; Wu, C. Z.; Liu, W. C. *Semicond. Sci. Technol.* **2001**, *16*, 997−1001.

(14) Butler, M. A. *Appl. Phys. Lett.* **1984**, *45*, 1007−1009.

(15) Wolfe, D. B.; Love, J. C.; Paul, K. E.; Chabinyc, M. L.; Whitesides, G. M. *Appl. Phys. Lett.* **2002**, *80*, 2222−2224.

(16) Kong, J.; Chapline, M. G.; Dai, H. *Adv. Mater.* **2001**, *13*, 1384−1386.

(17) Smith, P. A.; Nordquist, C. D.; Jackson, T. N.; Mayer, T. S.; Martin, B. R.; Mbindyo, J.; Mallouk, T. E. *Appl. Phys. Lett.* **2000**, *77*, 1399−1401.

(18) Huang, Y.; Duan, X.; Wei, Q.; Lieber, C. M. *Science* **2001**, *291*, 630−633.

(19) Ramanathan, K.; Bangar, M. A.; Yun, M.; Chen, W.; Mulchandani, A.; Myung, N. V. *Nano Lett.* **2004**, *4*, 1237−1239.

10.1021/cm048931n CCC: $27.50
Published on Web 10/27/2004

sions by combining electrodeposition and e-beam lithography.

The importance of a palladium nanowire was generated due to its ability to sense hydrogen gas with high sensitivity. The detection of hydrogen gas is important for fuel cell technology and environmental monitoring applications. The ability of the hydrogen atoms to occupy the octahedral interstitial positions within the palladium face-centered cubic (fcc) lattice structure forms the basis for this sensor. The incorporation of hydrogen atoms results in the formation of palladium hydride, leading to a change in the properties of the palladium metal, e.g., resistance/conductivity, grain size, and $\alpha-\beta$ phase transition.[20] This catalytic effect of palladium on hydrogen molecules is fast and reversible. Using this approach of a change in the grain size and/or resistance/conductivity of palladium, field effect transistors,[12,13] microelectronic sensors,[15] optical sensors,[14] mesowire-based hydrogen sensors and switches,[10] and carbon-nanotube-based sensors[16] have been constructed.

In this study we demonstrate the deposition of a nanodimension palladium wire as a hydrogen sensor using inexpensive electrochemical instrumentation. In the present work, we have systematically investigated the effect of various parameters on the electrodeposition of palladium nanowires from the solution phase onto prepatterned electrolyte channels. This technique offers an individually addressable palladium nanowire/array without the need for postsynthesis modifications/alignment of the nanowires. The electrodeposition technique involves growth of a nanowire in an electrolyte channel between the gold electrodes, which are fabricated by e-beam lithography and lift-off techniques. A nanosensor array can be fabricated by introducing electrolyte into each channel, allowing the electrodeposition of nanowires individually or simultaneously. This technique enables easy fabrication of a ready to use, individually addressable nanowire sensor array with the capability of simultaneously detecting multiple chemical species. Optimization of different parameters has been achieved to obtain true palladium nanowires of less than 100 nm width.

Experimental Section

As reported earlier,[9] electrodes were fabricated on a (100)-oriented silicon wafer with a chemical vapor deposition (CVD) grown 1 μm thick insulator layer of low-stress Si_3N_4 film. A Cr adhesion layer and a ~3000 Å thick Au contact layer were then deposited, with contacts being patterned by lift-off. Thermally evaporated SiO was then deposited on the wafer at room temperature followed by a coat of PMMA photoresist. Using e-beam lithographic patterning, the deposited SiO and PMMA were selectively opened with reactive ion etching to form electrolyte channels. The widths of the electrolyte channels were fixed at 100, 200, 500, or 1000 nm (Figure 1A).

As shown in Figure 1B, 2 μL of the metal ion electrolyte was placed on top of each channel with a microliter syringe. Alkaline palladium p-salt electrolyte solution consisting of 10 g/L $Pd(NH_2)_2(NO_2)_2$ and 100 g/L ammonium sulfamate was used for electrodeposition of the palladium nanowires. The pH of the solution was adjusted to 8.0 by addition of sulfamic acid and sodium hydroxide. This optimized electrolyte composition was important to prevent hydrogen gas evolution and dissolution of the Cr adhesion layer, which is readily attacked by the acidic environment.

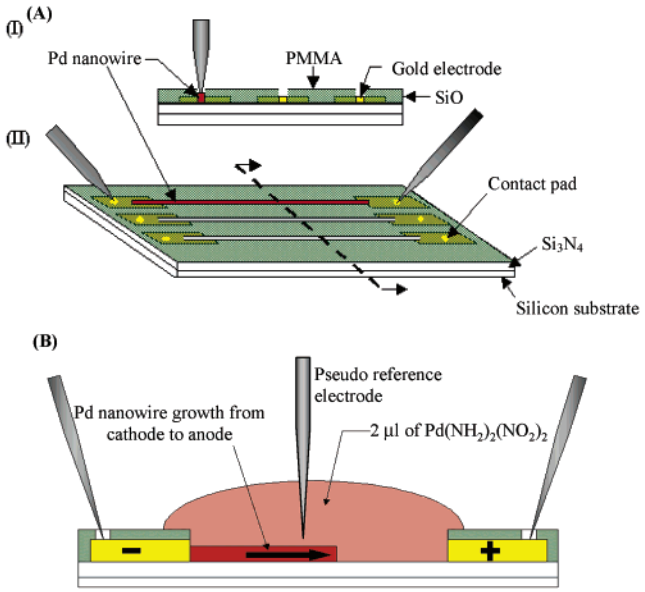

Figure 1. (A) Schematic of e-beam lithographically patterned electrolyte channels with defined channel dimensions, showing cross-sectional details (I) and the electrode arrangement in an array (II) with individually addressable electrolyte channels. (B) Electrodeposition process: a 2 μL drop of an electrolyte solution of Pd salt (10 g/L) is placed on the channel between the gold electrodes, and the electrodeposition of the Pd nanowire takes place from the cathode to the anode under galvanostatic conditions.

A nanowire is electrodeposited under both a potentiostatic (i.e., constant applied potential) mode and a galvanostatic (i.e., constant applied current) mode. In the case of a galvanostatic growth, initiation and the growth of the nanowire is monitored using a chronopotentiogram and terminated as the potential value drops to ~0 V. The applied currents were varied from −25 to −600 nA. In the case of a potentiostatic mode, initiation and growth of the nanowire is monitored by continuous measurement of the resistance between the electrodes and terminated as the resistance value drops from a few thousand to a few hundred ohms. The applied potential was 1.5 V between the cathode and the anode.

The deposition was carried out at 25 °C and ambient pressure. The nanowire growth was initiated from the cathode toward the anode through the electrolyte channel when an electric current was applied using Biologic Science Instrument's (Princeton Applied Research) VMP2 multichannel potentiostat/galvanostat. The dimensions of the wire were predetermined by the width of the channel and the distance between the electrodes. The channel also restricted the dendritic growth of the palladium nanowire. To characterize the growth, the resistance change as a function of deposition time was monitored by using a multimeter (HP 34401A Multimeter) during the deposition of the nanowire within the channel. The nanowires were characterized by optical microscopy (high-resolution Hirox videomicroscope 7000X) and scanning electron microscopy (SEM) (Philips XL30-FEG) and by recording the current versus voltage ($I-V$) response to determine the nanowire resistance.

Results and Discussion

The electrodeposition process was initiated by placing a 2 μL drop of the palladium salt solution on the electrode surface (Figure 1B). The hydrophobic nature of the PMMA photoresist prevented the drop from spreading on the surface of the chip. The pseudo reference electrode in contact with the drop enabled the

(20) Lewis, F. A. *Int. J. Hydrogen Energy* **1995**, *20*, 587−592.

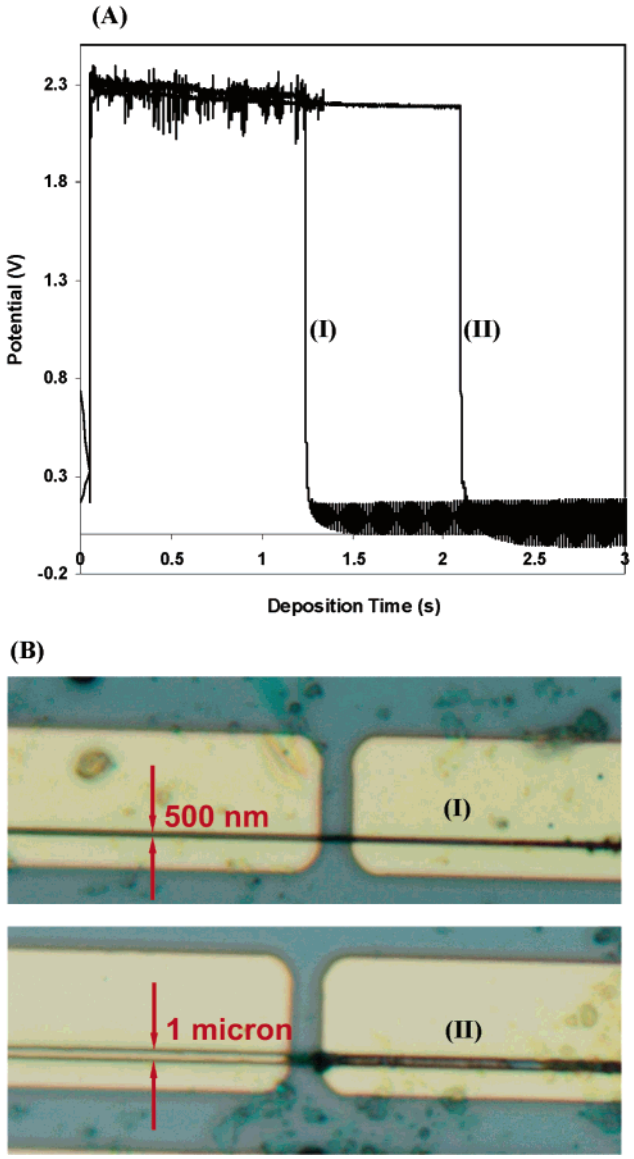

Figure 2. (A) Chronopotentiograms recorded for the Pd nanowires grown under the galvanostatic mode at −50 nA using 500 nm (I) and 1 μm (II) channel widths. (B) Optical images using 7000× magnification (reproduced at 81% of the original size) of Pd nanowires grown in 500 nm (I) and 1 μm (II) wide channels.

monitoring of the potential changes on the surface of the cathode. The palladium p-salt solution fills the channel and establishes contact between the gold electrodes. Incorporation of the solution into the channel is probably dependent on the interfacial tension between the electrolyte solution and the channel surfaces in addition to the capillary action of the channel. The presence of air bubbles may interfere during nanowire formation. Figure 2A shows typical chronopotentiometric responses recorded during the growth of a palladium nanowire under the galvanostatic mode of electrodeposition. Upon application of a −50 nA current step, the potential of the cathode increased from the open circuit voltage of 0.0−0.8 V to about 2.2−2.3 V with respect to the reference electrode. The observed value of the open circuit voltage developed may be attributed to nonelectrochemical processes such as adsorption of ions on the electrode surface, charge interactions with the electrode, and the buildup of a charge bilayer on the gold electrode

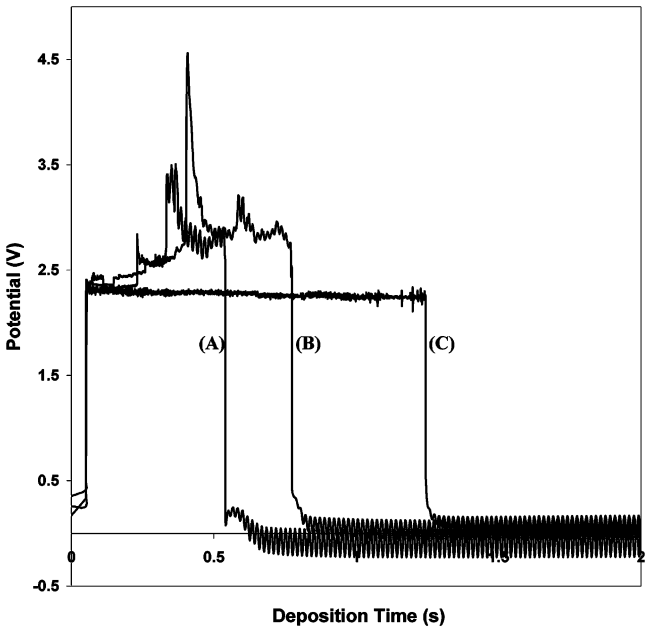

Figure 3. Chronopotentiograms for Pd nanowires grown under the galvanostatic mode at −200 nA (A), −100 nA (B), and −50 nA (C) applied currents within 500 nm wide channels.

surface, which reflects the initial Pd^{2+}/Pd concentration in the electrolyte solution.

As the growth of the nanowire progresses from the cathode to the anode, the newly formed nanowire starts acting as the cathode. It leads to a decrease in the interelectrode gap between the cathode and the anode and was indicated by the downward slope of the chronopotentiograph. It also reflects the continued conversion of Pd^{2+} to Pd at the cathode. This reduction reaction takes place at a potential of the working electrode of 2.2−2.3 V with respect to the pseudo reference electrode. However, the passage of current between the electrodes is via charge conduction through the solution phase. As the nanowire growth reaches the anode, the potential drops to ∼0 V. This could be attributed to a flow of current through the more conducting metallic Pd nanowire as opposed to the lower solution-phase conductivity. At this stage the majority of the current flow is through the Pd nanowire. The subsequent change in the potential around 0.0 V is probably due to electrode processes following nanowire formation. Under the galvanostatic mode of electrodeposition the deposition rate was controlled at a fixed value by maintaining a constant current density. Thus, a change in the channel width from 500 nm (Figure 2A, curve I) to 1 μm (Figure 2A, curve II) resulted in an increase in the deposition time from 1.3 to 2.2 s, respectively, at the same applied current, indicating that additional deposition of Pd ions is required to form a nanowire connecting the two gold electrodes which were ∼2.5 μm apart. The deposition of the palladium nanowire was initiated within the channel on the gold surface followed by filling up of the channel between the electrodes, resulting in the formation of uniform and well-confined nanowires as elucidated in Figure 2B (I and II).

For a fixed channel width (500 nm) the rate of deposition varied with a change in the applied current from −50 to −200 nA (Figure 3). At higher current (−200 nA, Figure 3, curve A) the rate of deposition is

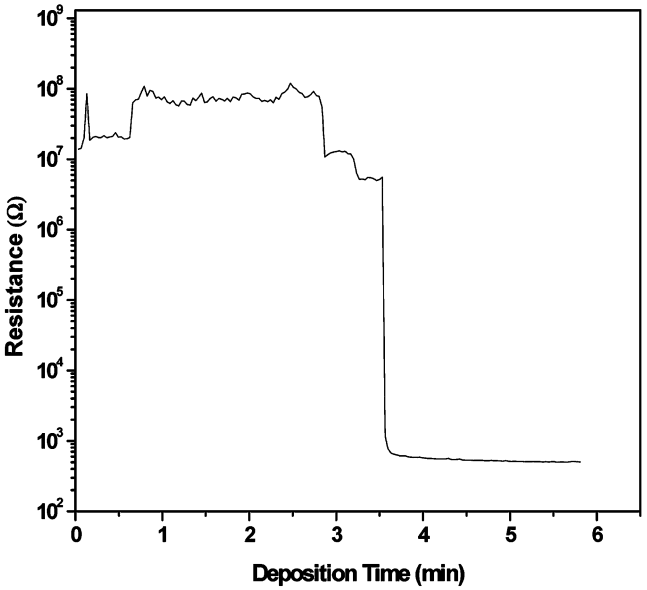

Figure 4. Resistance changes from 10^8 to ~500 Ω during the growth of a Pd nanowire under the potentiostatic mode at 1.5 V between the cathode and the anode.

higher, leading to a faster nanowire formation (0.5−0.6 s). Alternatively, at a −50 nA current step the nanowire is formed in about 1.3 s (Figure 3, curve C), while it is formed in about 0.75 s for a −100 nA current step (Figure 3, curve B). The results suggest that a shorter time period is required to deposit a fully connected palladium nanowire at a higher deposition rate for a defined channel width. At applied currents higher than −200 nA, partial discoloration of gold electrodes was observed, probably resulting from the overheating of the electrodes, although directional control over growth was improved. In addition, the resistance values for nanowires grown using applied currents higher than −200 nA showed significant variation (data not shown).

In contrast, deposition currents lower than −50 nA led to overdeposition outside the channel, indicating poor directional control over growth. At lower currents the deposition tends to fill the entire cross section of the channel probably due to deposition in the radial direction, whereas at higher currents preferential longitudinal growth takes place wherein deposition tends to fill the interelectrode gap rather than the cross-section of the channel. As a result, at higher applied currents the nanowire width was less than the channel width used for electrodeposition, indicating a differential distribution of current density at the cross-sectional area of the nanowire compared to its longitudinal surface area. Thus, the molecules show a stronger tendency to deposit at the deposition front of the growing nanowire at higher applied currents compared to lower currents. The current density also affects the morphology of the nanowire. The nanowires grown at lower applied currents have a smooth surface texture, whereas the nanowires grown at higher currents look like a chain of beads linked together. However a −100 nA applied current provided well-defined palladium nanowires with high yield on a consistent basis.

In addition to the galvanostatic mode of electrodeposition, we also electrodeposited palladium nanowire using a potentiostatic mode by applying a fixed potential of 1.5 V between the cathode and the anode. In this case,

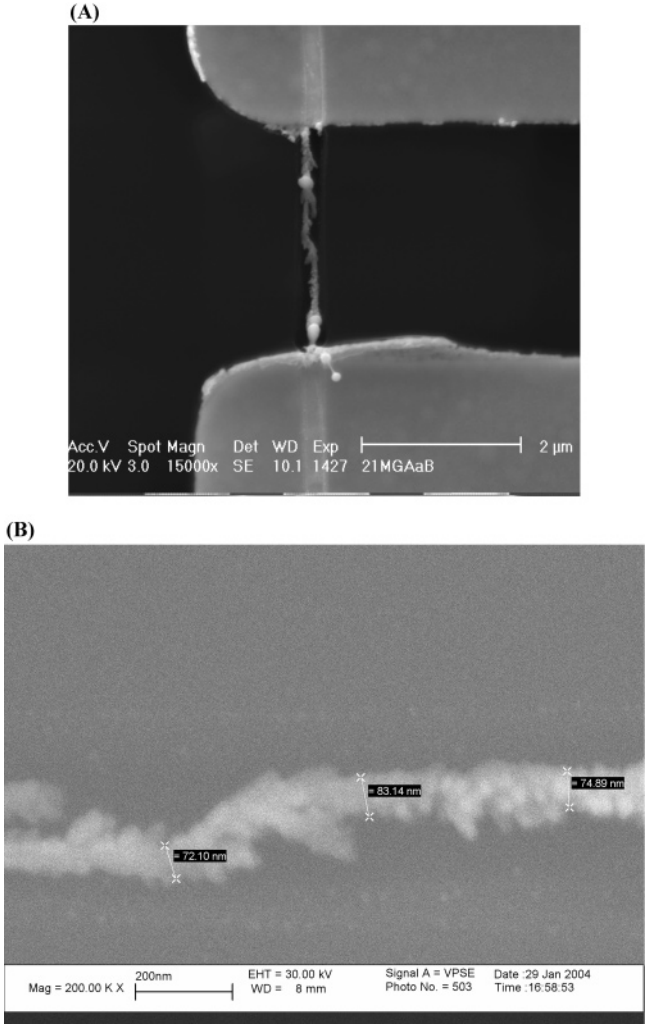

Figure 5. SEM images of an electrodeposited single palladium nanowire of approximately 80 nm diameter and 2.5 μm length under 15000× (A) and 200000× (B) magnifications (reproduced at 68% of the original size).

the resistance changes between the gold electrodes during the growth of a palladium nanowire (100 nm) were monitored (Figure 4). The resistance between the electrodes was initially in the 10−100 MΩ range, followed by a stepwise decrease in resistance during the growth of the palladium nanowire. As the nanowire established contact with the gold electrodes the resistance dropped and reached a plateau at ~500 Ω. A slow rate of decrease in the resistance was observed thereafter in the presence of the electrolyte. The resistance value remained stable for several hours following the growth and the removal of the electrolyte, an observation consistent with the presence of a conducting nanowire. An SEM image of a potentiostatically grown single palladium nanowire with a channel diameter of 100 nm is shown in Figure 5A. The image illustrates the well-confined deposition of the nanowire within the channel and the absence of any dendritic growth outside the channel. The nanowire is 2.5 μm in length between the cathode and the anode. A higher magnification SEM micrograph showed the diameter of the nanowire ranged between 72 and 84 nm (Figure 5B).

To characterize the electrical properties of nanowires, $I-V$ profiles were recorded on the palladium nanowire in the presence (wet condition) and absence (dry condi-

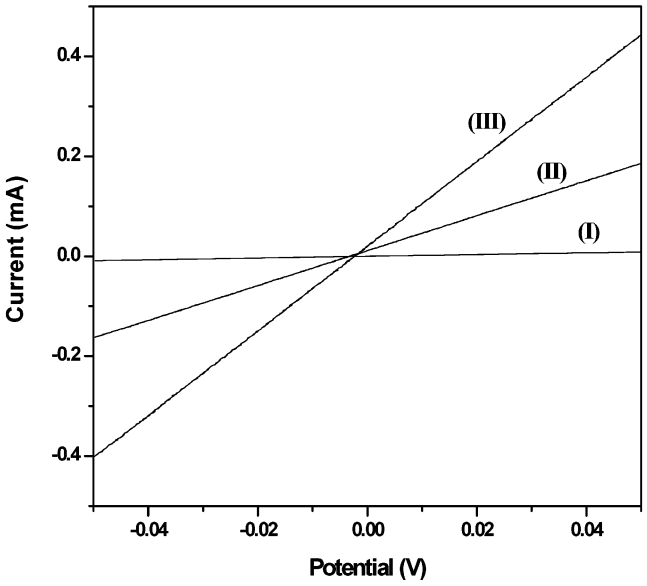

Figure 6. $I-V$ profiles for Pd nanowires grown within 100 nm (I), 500 nm (II), and 1 μm (III) wide electrolyte channels under the dry condition, between −0.05 and 0.05 V at a scan speed of 50 mV/s.

tion) of the electrolyte solution. The nature of the $I-V$ profiles remained unchanged in the presence or absence of electrolyte. The straight-line nature of the $I-V$ response under the dry condition (Figure 6) confirms the ohmic behavior of the nanowire with the gold electrodes. As expected, with a reduction in the cross-sectional area or the width of the channel, the resistance (inverse of the slope of the $I-V$ lines) of the nanowire increased (Figure 6, lines I−III). From the resistivity calculations, palladium nanowires showed a higher resistivity of 10^{-6} Ω·m as compared to its bulk resistivity value of about 10^{-7} Ω·m. As reported in an earlier work,[9] the higher value of resistivity may be attributed to a smaller grain size. As the grain size decreases, the density of the grain boundaries increases, offering a greater resistance to the flow of current.

Conclusion

We demonstrated the growth of palladium nanowires and investigated the effect of different deposition variables on its growth. The growth conditions were optimized to obtain true individually addressable palladium nanowires with controlled dimensions on e-beam-patterned electrolyte channels. Nanowires with a diameter of less than 100 nm were fabricated using a palladium salt solution as the electrodeposition medium. The nanowire formation was confirmed using optical, SEM, and electrical measurements. The technique of electrodeposition offers a fast and single-step method of making palladium nanowires without the need for a tedious postgrowth assembly. The results confirm that the galvanostatic method offers control over directional growth and the deposition rate. It was also shown that an applied current of −100 nA provided an optimum current density for obtaining good-quality palladium nanowires. Changes in the morphology of the nanowire with the variation in the applied current density were also investigated. The nanowires showed ohmic behavior with gold electrodes with an increase in resistivity at decreased grain size.

We are currently investigating the utility of different electrolytes to fabricate a sensor array consisting of nanowires of different materials. Such arrays can offer potentially different chemical-sensing capabilities using the same platform. It is envisioned that these are the initial steps toward the fabrication of nanowire sensor arrays capable of simultaneously detecting multiple chemical species.

Acknowledgment. We acknowledge Liqun Chen for performing a few of the experiments. We also acknowledge the support of this work by DOD/DARPA/DMEA under Grant Number DMEA90-02-2-0216, the Center for Nanoscale Innovation for Defense, the and NASA Code R Bio/Nano Program. The Jet Propulsion Laboratory is an operating division of the California Institute of Technology and is under a contract with the National Aeronautics and Space Administration.

CM048931N